Progress In Electromagnetics Research M, Vol. 119, 51–62, 2023

Investigation on Performance of Four Port MIMO Antenna Using Electromagnetic Band Gap for 5G Communication

Govindarao Tamminaina* **and Ramesh Manikonda**

Abstract—In order to support 5G communication, this article suggests a small, four-port MIMO antenna with a G slot. This antenna has an electromagnetic band gap (EBG) in the shape of an S that is engraved on the substrate in the space between consecutive pairs of radiating patches. The recommended MIMO antenna is constructed from an FR4 substrate and measures $48 \times 48 \times 1.6\,\text{mm}^3$. Between antenna elements 1 and 2, the integrated EBG structure of the MIMO antenna can reduce mutual coupling by 10.5 dB. The suggested four port G slot MIMO antenna with an S-shaped EBG structure displays the performance in terms of ECC less than 0.0002 and diversity gain larger than 9.99 with consistent frequency band extending from 3.3 GHz to 3.7 GHz. The proposed four port MIMO antenna is designed using HFSS software, and its simulation results are measured using anritsu combinational analyzer MS2037C vector network analyzer.

1. INTRODUCTION

The demand for multiple-input multiple-output (MIMO) systems has expanded in the modern period for wireless applications. It shows better performance in fading environment and also supports high data rate. Designing a two-element isolation-improved MIMO antenna that can operate between 4.04 GHz and 5.48 GHz for 5G applications is the goal of the study [1]. Two antenna components that are kept at the substrate's outermost edges and have dimensions of $100 \times 50 \times 0.8\,\text{mm}^3$ make up the MIMO arrangement. The use of a metasurface between MIMO antenna components provides outstanding isolation (-23 dB) witnessed by the current distribution on surface of antenna. A significant barrier to using the MIMO antenna's best performance is the mutual coupling of undesired fields between the components.

In the 2.4 GHz frequency range, a portable four-element self-isolated MIMO antenna is shown [2] for Industrial, Scientific, and Medical (ISM) applications. Four printed dipoles make up the suggested design; therefore these antennas will be fed by four integrated baluns. Great isolation is attained in the first phase by utilising the capability of self-isolated antennas. The proposed MIMO antenna's constructed prototype functions in 2.2 and 2.87 GHz frequency range and achieves the isolation more than 19 dB and envelope correlation coefficient (ECC) of less than 0.0009. A new decoupling structure is integrated with a compact 6 ports ultra-wideband (UWB) antenna [3], and port-to-port isolation is analysed to improve the port isolation. The suggested design's unique decoupling structure was made up of parasitic parts and six UWB antennas with symmetrical pyramidal shapes and distributed flawed ground constructions.

This study [4] offers a simulated analysis of a four port MIMO antenna design that supports 5G mobile technologies by using meandered-line folding. The $150 \times 75\,\text{mm}^2$ main board of a mobile phone with a defective grounded structure (DGS) on its horizontal surface serves as the foundation for the suggested MIMO system. Operating at 3.5 GHz, the suggested MIMO antenna system has the isolation

Received 3 August 2023, Accepted 2 September 2023, Scheduled 14 September 2023
* Corresponding author: Govindarao Tamminaina (gtammina@gitam.in).
The authors are with the Department of ECE, GITAM University, India.

of more than 20 dB. While the new DGS enhances isolation between antennas, the meandered-line folding structure helps to decrease the area of antennas. A dual polarized aperture antenna with a triple-band construction is recommended in [5] for the usage in 5G base station applications. MIMO antennas are designed for the triple bands, 0.69–0.96 GHz, 1.8–2.7 GHz, and 3.3–3.8 GHz, respectively. To lessen the impact of lower band (LB) on mid-band (MB) and high band (HB), a wideband band-stop frequency selective surface (FSS) is utilized. The suggested antenna has gains of 6.5, 7.6, and 8.2 dB in the low, mid, and high bands, respectively, based on observed data.

A planar Inverted-F antenna with an open slot in an Inverted-T configuration is seen in the letter [6]. The suggested antenna resonates with a broad bandwidth of 78% because of multi-mode technology. Then, a planar inverted F-shape antenna (PIFA)-pair is constructed to provide a 2×2 MIMO antenna, and it has a broadband isolation between them of larger than 10 dB. The antenna correlation coefficient (ACC) matrix is used in [7] to determine the performance indicators. The ACC matrix's rank is used to compute the diversity order (DO), and its trace and frobenius norm are used to determine the diversity measure (DM).

A compact, highly isolating MIMO antenna made for the fifth-generation (5G) smart phones uses a chip capacitive decoupler [8] to promote the isolation between the two feeding ports. Further modifications to the isolation between the modules are made using spiral slots. It consists of a chip capacitive decoupler, two feeding ports, and metal strips that radiate heat. In order to make the module smaller, two L-shaped metal strips are used in this design as distributed capacitors. A 4-port substrate integrated gap waveguide (SIGW)-based MIMO antenna for down-link satellite applications is shown in [9]. The suggested MIMO antenna, provided by SIGW, has four rectangular radiating slots and reduces insertion loss and dispersion with a constant radiation pattern spanning the 13.4–13.65 GHz bandwidth.

A dual-polarization microstrip MIMO antenna is shown in [10] for the use in 5G mobile phone applications. The back cover of a mobile phone is equipped with eight fed microstrip antenna components. Four shorted radiation patches comprise an antenna pair's radiator, whereas four radiators make up an eight-element MIMO antenna. The interaction between the two components of one antenna pair allows the antenna element, which has a wide working band, to excite two modes. Eight power dividers are used to create a MIMO antenna prototype and supply the differential feeding. A MIMO antenna array with eight antenna elements and four antenna elements is created for low specific absorption rate (SAR) in [11, 12] for 5G mobile phones with −6 dB ranges from 3.4 to 3.6 GHz. Theory of characteristic mode (TCM) is first used to evaluate a dipole antenna with geometric symmetry. The modal currents with 5G wireless networks in FR1 and FR2 frequency bands are examined in [13] to construct the low-SAR antenna element. A survey is made on different techniques to enhance the coverage of 5G wireless systems [14]. In [15], a MIMO antenna is designed with dielectric resonator, electromagnetic bandgap (EBG), and defected ground structure (DGS) techniques. Similar to DGS, EBG will enhance the performance of huge MIMO antennas for applications in the −6 GHz range.

2. DESIGN METHODOLOGY OF MIMO ANTENNA

2.1. Design of Single Patch Antenna

The rectangular microstrip patch antenna's design parameters length and width are initially computed using the following formulae [16]; after that, the dimensions are optimized using parametric analysis in HFSS software, and the parameters are improved for better outcomes.

$$W = \frac{v_o}{2f_r}\sqrt{\frac{2}{\varepsilon_{r+1}}} \tag{1}$$

$$\varepsilon_{reff} = \frac{\varepsilon_r + 1}{2} + \frac{\varepsilon_r - 1}{2}\left[1 + 12\frac{h}{W}\right]^{-1/2} \tag{2}$$

$$\frac{\Delta L}{h} = 0.412\frac{(\varepsilon_{reff}+0.3)\left(\frac{W}{h}+0.264\right)}{(\varepsilon_{reff}-0.258)\left(\frac{W}{h}+0.8\right)} \tag{3}$$

$$L = \frac{v_0}{2f\sqrt{\varepsilon_{reff}}} - 2\Delta L \tag{4}$$

The patch's length and width are indicated by letters L and W. The letters h and ε_r, respectively, stand for the substrate's height and relative permittivity. ε_{reff} is the effective permittivity, f_r the resonant frequency, ΔL the length extension on each end, and v_0 the velocity of light.

The G slot is initially made on a rectangular single patch antenna which is designed on a substrate of FR4 with a faulty ground structure and $\varepsilon_r = 4.4$, 1.6 mm height. Figures 1(a) and 1(b) depict the G slot single patch antenna's dimensions from the front and back, respectively. Figure 1(c) shows the isometric view of the proposed single-patch antenna.

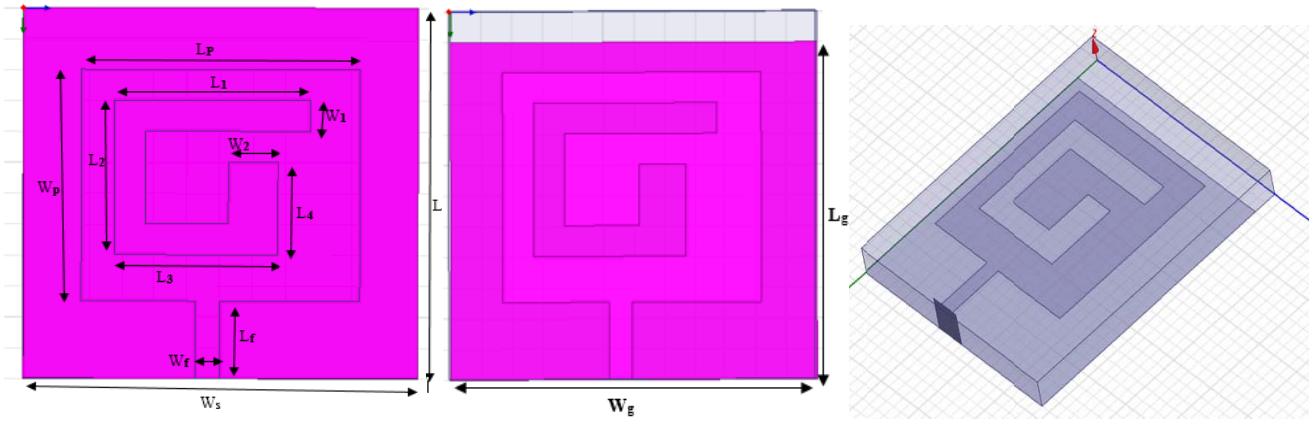

Figure 1. Schematic view of the single patch antenna. (a) Front and (b) back, (c) isometric.

Table 1 displays the design specifications for the G slot single patch antenna. The parameters are optimized using parametric analysis of HFSS software.

Table 1. The specifications for the proposed structure.

Parameter	L_g	W_g	L_s	W_s	L_p	W_p	L_f	W_f	L_1	L_2	L_3	L_4	W_1	W_2
Value (mm)	22	24	24	24	15	17	5	1.5	12	10	10	6	2	3

The reference antenna is analysed while changing the length of the ground (L_g) using parametric analysis technique. The L_g value is changed from 19 mm to 24 mm, which is shown in Figure 2.

Figure 3 displays the G slot patch antenna's reflection coefficient. The antenna is resonant from 3.3 to 3.7 GHz with $S_{11} < -10$ dB value being 29.7 dB.

2.2. Design of MIMO Antenna

The four port G slot MIMO antenna is implemented using a reference antenna. The four antennas are arranged orthogonal to each other. Figure 4(a) shows the front view, and also port numbers are mentioned in that diagram. The back view of the four port MIMO antenna with a flawed ground structure is depicted in Figure 4(b).

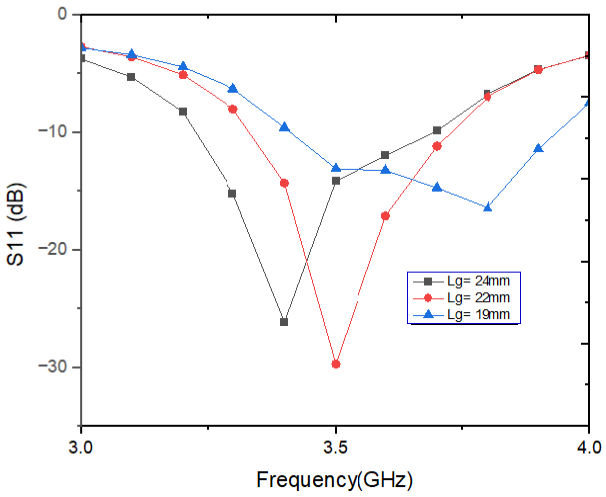

Figure 2. Reflection coefficient of reference antenna using parametric analysis.

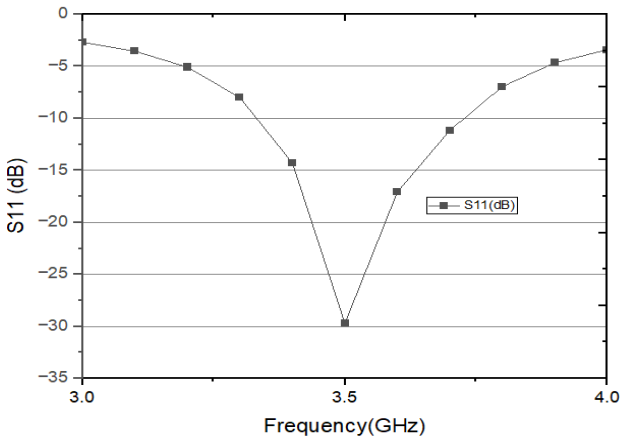

Figure 3. S_{11} of reference antenna.

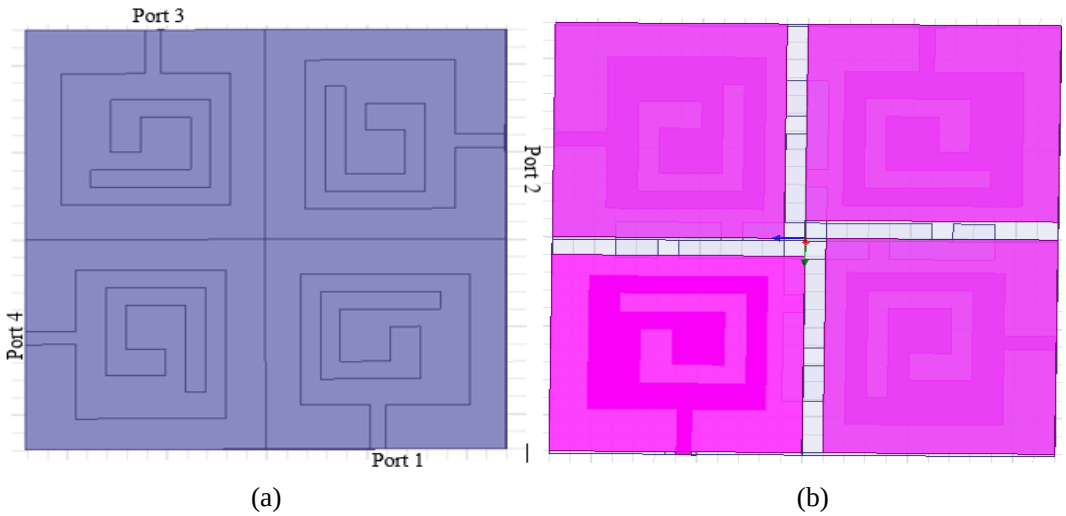

Figure 4. (a) Front view of a MIMO antenna and (b) back view.

Figure 5 displays a four port MIMO antenna that is integrated with an EBG construction. The suggested antenna is 48 mm in length (L_o) and 48 mm in width (W_o) overall. Here, four S-shaped EBGs are arranged between four antennas. The dimensions of S-shaped EBG is $L_e = 16$ mm and $W_e = 4$ mm. The EBG structure is implemented with copper material.

Figure 6(a) depicts the front view of the four port MIMO antenna with an S-shaped EBG structure, and Figure 6(b) depicts the back view with a flawed ground structure.

3. RESULTS AND DISCUSSIONS

Figure 7 depicts the design parameters for the S-shaped EBG structure. Here, dimensions of substrate are $L_b = 20$ mm, $W_b = 10$ mm; height is 1.6 mm; and FR4 is a substrate material. For S-shaped EBG, the dimensions of patch are $L_e = 16$ mm, $W_e = 4$ mm, and slots are $L_m = 2$ mm, $L_n = 2$ mm, and $W_n = 2$ mm.

Figure 8 depicts the S-shaped EBG structure's reflection phase as a function of frequency. The reflection phase varies between 90° and −90° for a frequency range 3.3 GHz to 3.7 GHz. It lessens the

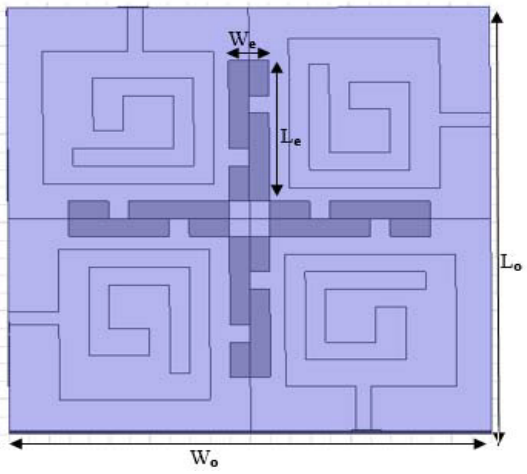

Figure 5. An EBG structure and MIMO antenna.

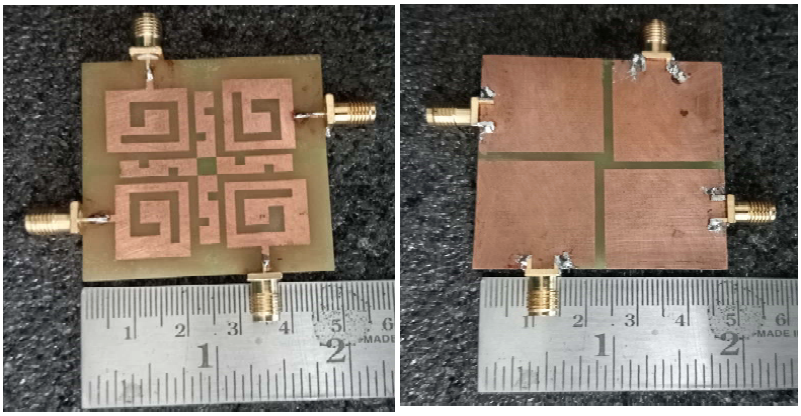

(a) (b)

Figure 6. MIMO antenna with G slots fabricated views of the (a) front and (b) back.

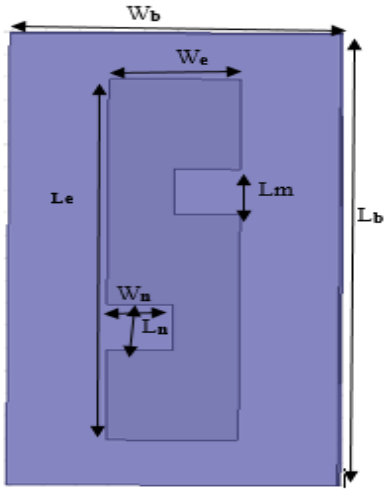

Figure 7. Schematic view of EBG cell.

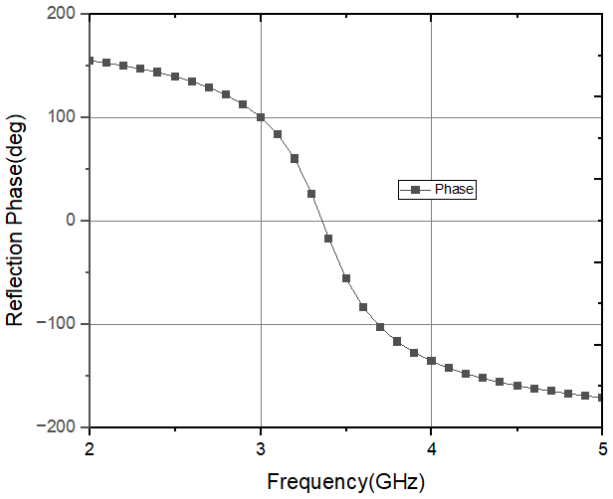

Figure 8. Reflection phase of S-shaped EBG structure.

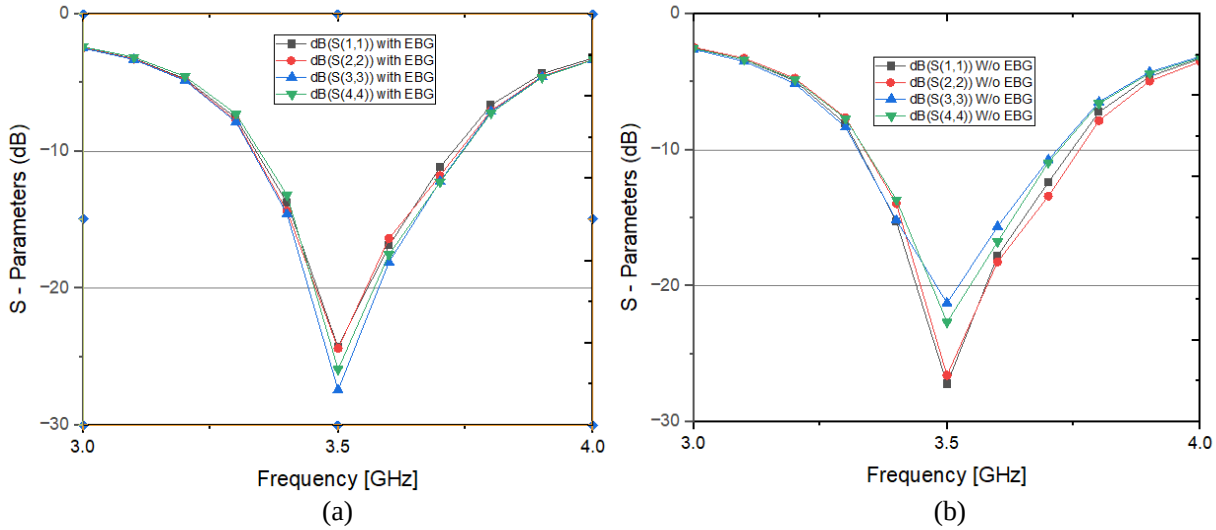

Figure 9. Simulations of the proposed MIMO antenna's S-parameters (a) with EBG, (b) without EBG.

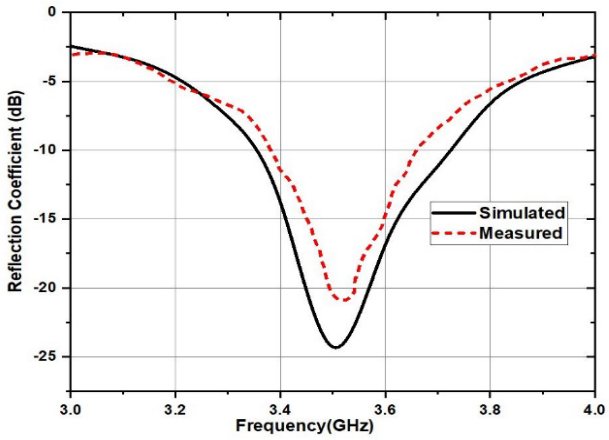

Figure 10. Reflection coefficient of MIMO antenna with EBG structure.

impact of surface waves within a band gap.

Figure 9 shows the reflection coefficients of four port G slot MIMO antenna at different ports 1, 2, 3, and 4. Figure 9(a) is with S-shaped EBG and Figure 9(b) without EBG structure. The EBG structure has a smaller impact on the MIMO antenna's reflection coefficient.

The measured and simulated reflection coefficients (S_{11}) of G slot four port MIMO antenna embedded with S shaped EBG structure are presented in Figure 10.

Figure 11 shows the transmission coefficients of four port G slot MIMO antenna with and without S-shaped EBG structure. It can be seen that when there is no EBG structure, the result of S_{12} is -27.5 dB. By inserting an S-slot EBG structure, at 3.6 GHz, the S_{12} value drops to -38.0 dB, which decreases the antennas' mutual coupling. This demonstrates the improved port isolation for a four port MIMO antenna built utilizing an EBG.

Figure 12 compares the transmission coefficients at the various ports S_{12}, S_{13}, and S_{14} of a MIMO antenna with an S-shaped EBG structure between simulations and measurements.

The surface current distribution of a four port G slot MIMO antenna with an S-shaped EBG structure is shown in Figure 13(a) at 3.5 GHz and 13(b) at 3.6 GHz. The effect of mutual coupling between different ports is reduced due to the EBG structure. The LC resonance circuit's resonance

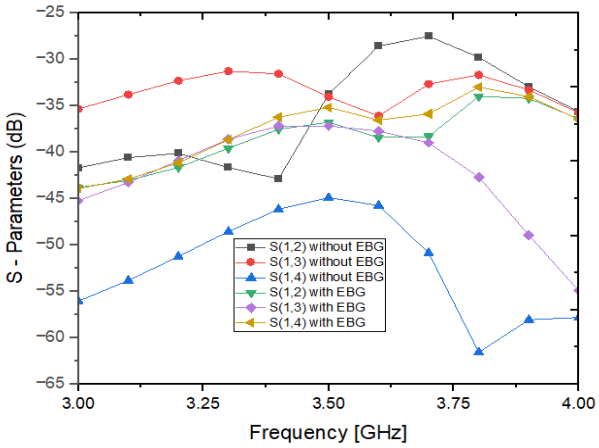

Figure 11. Transmission coefficient of MIMO antenna.

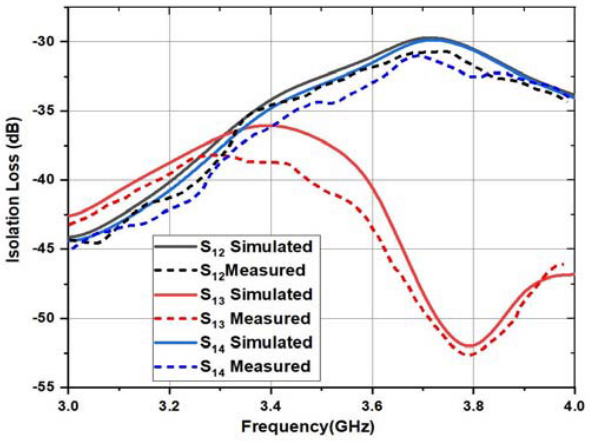

Figure 12. Measured transmission coefficient of MIMO antenna with EBG.

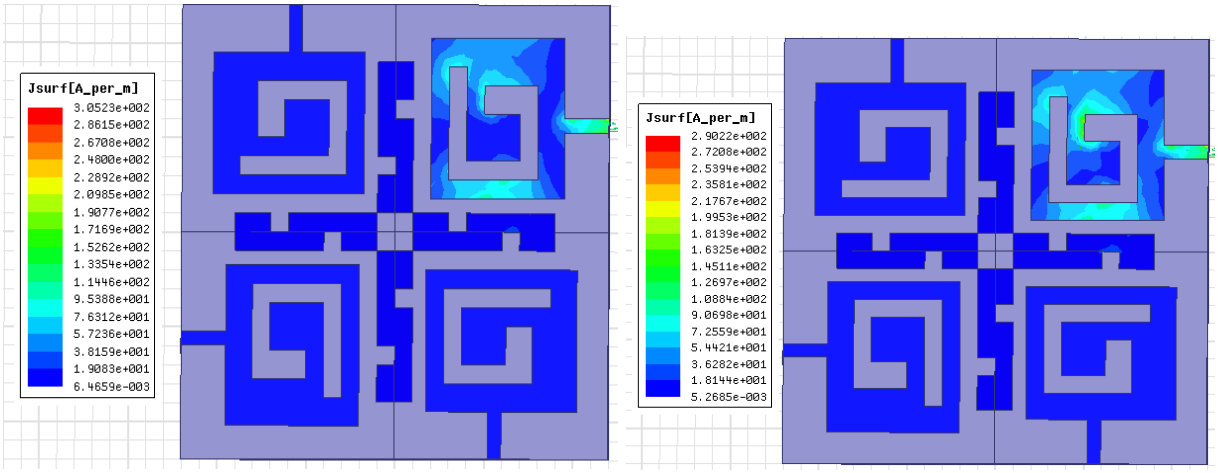

Figure 13. MIMO antenna surface current distribution with EBG at (a) 3.5 and (b) 3.6 GHz.

frequency causes the high-impedance electromagnetic surface to resemble a filter, preventing current from flowing on the conductor's surface and suppressing surface wave propagation. Thus, at the resonance frequency, a surface wave band gap is created.

The radiation pattern of four port G slot MIMO antenna with an S-shaped EBG structure is shown in Figure 14(a) at 3.5 GHz and 14(b) at 3.6 GHz. The S-shaped EBG structure is designed to reduce the effect of the surface wave for a desired frequency band. Then, it improves the antenna gain and reduces the backward radiation.

3.1. MIMO Antenna Parameters

Equation (5) contains the value of the Envelope Correlation Coefficient (ECC), which was computed using the S parameters equation [17].

$$\mathrm{ECC} = \frac{\left|S_{ii}^{*}S_{ij} + S_{jj}^{*}S_{ji}\right|^{2}}{\left(1 - |S_{ii}|^{2} - |S_{ij}|^{2}\right)\left(1 - |S_{ij}|^{2} - |S_{jj}|^{2}\right)} \tag{5}$$

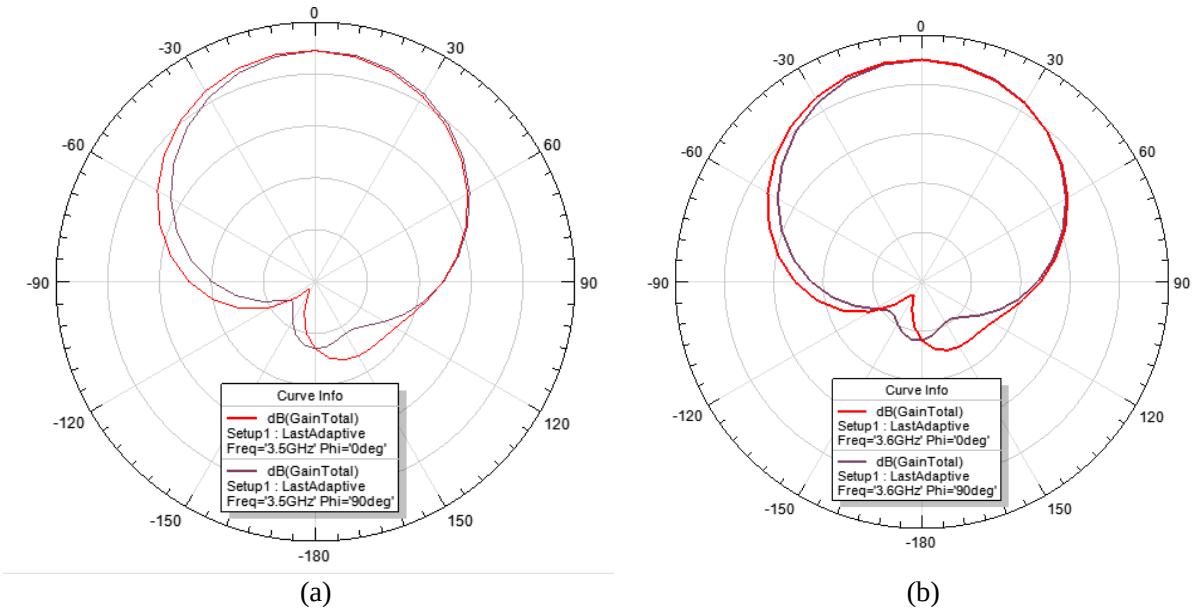

Figure 14. G slot MIMO antenna radiation pattern with S shaped EBG at (a) 3.5 GHz, (b) 3.6 GHz.

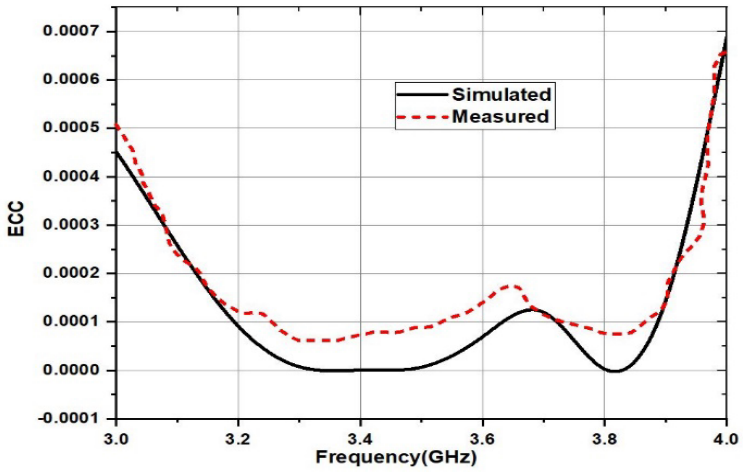

Figure 15. ECC of MIMO antenna with EBG.

The observed and simulated ECC values for the four port G slot MIMO antenna with an EBG structure are less than 0.0002 in Figure 15, which is below the permissible threshold.

The values of the S parameters are used to determine the diversity gain of the proposed MIMO antenna and provided in the equation below.

$$\mathrm{DG} = 10\sqrt{1 - (\mathrm{ECC})^2} \tag{6}$$

The diversity gain of the MIMO antenna with the EBG structure is shown in Figure 16. Both the measured and simulated values for the target frequency band are greater than 9.99.

Figure 17 depicts the four port MIMO antenna with an S-shaped EBG's simulated and observed efficiencies, which for the suggested frequency band is greater than 77%.

Figure 18 displays the four port MIMO antenna's simulated and observed gains for the S-shaped EBG structure. At 3.6 GHz, the maximum simulated value is 3.3 dB.

Another crucial component of the MIMO antenna is the TARC (Total Active Reflection Coefficient),

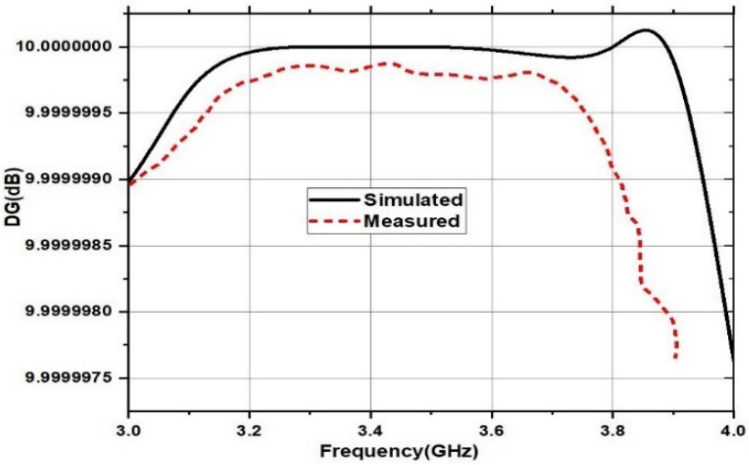

Figure 16. MIMO antenna diversity gain with EBG.

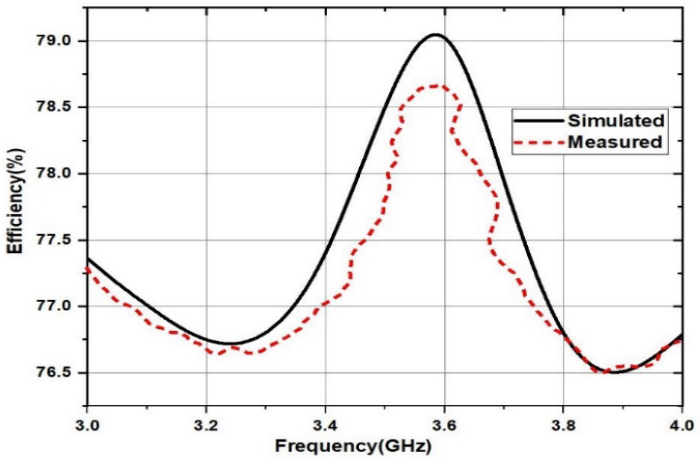

Figure 17. Efficiency of MIMO antenna with EBG.

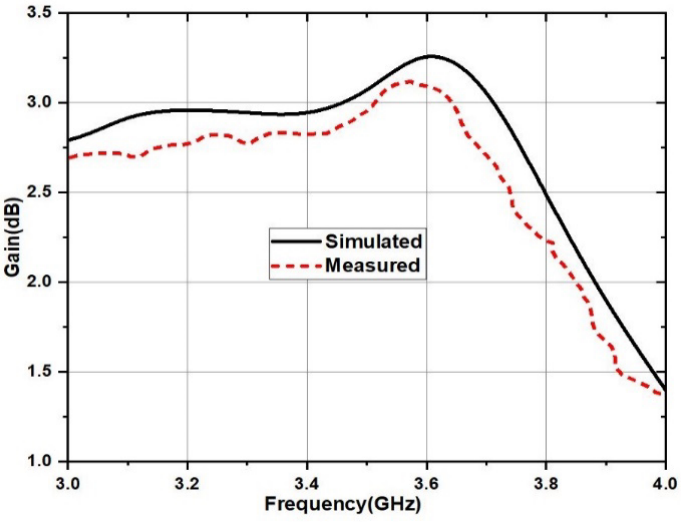

Figure 18. Gain of MIMO antenna with EBG.

which is determined using the equation below.

$$\text{TARC} = \frac{\sqrt{\left(|S_{ii} + S_{ij}e^{j0}|^2\right) + \left(|S_{ji} + S_{jj}e^{j0}|^2\right)}}{\sqrt{2}} \tag{7}$$

The simulated TARC of the MIMO antenna with EBG is shown in Figure 19. The TARC value typically falls between 0 and 1. Therefore, the simulated TARC value is less than 0.29. Table 2 shows the comparisons of different MIMO antenna parameters.

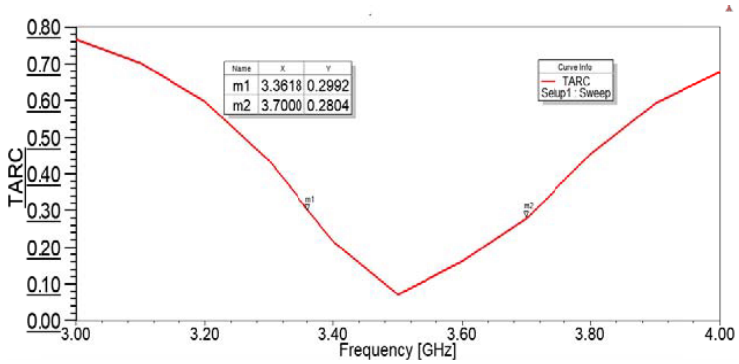

Figure 19. TARC of an EBG-equipped MIMO antenna.

Table 2. Comparison of proposed MIMO antenna and with other antennas.

Ref.	No. of elements	Antenna size (mm^2)	Operating bands (GHz)	Isolation (dB)	ECC	Efficiency (%)
[18]	8	72×72	4.4–5.5	−22	0.068	50
[19]	4	150×75	3.4–3.6	−17	0.1	58
[20]	8	150×63	3.33–3.73	−24	0.01	60
[21]	8	21.8×7	3.3–5	−26	0.18	71
[22]	4	53×20	3.8–8.3	−45	0.005	80
[23]	4	52×20	3.3–3.7	−20	0.05	80
[24]	8	150×75	3.1–6.2	−12	0.035	80
[25]	2	48×35	2.3–11.5	−34	0.07	85
[26]	2	30×60	3–12	−25	NA	90
[27]	2	58×58	2.4–4.6	−42	0.0025	92
Prop. Ant	**4**	**48×48**	**3.3–3.7**	**−10.5**	**0.0002**	**77**

4. CONCLUSION

The proposed S-shaped EBG based four port G slot MIMO antenna is compact in size ($48 \times 48 \times 1.6\,mm^3$). It has the necessary 5G NR frequency band (n78) with an $S_{11} < -10$ dB covering 3.3 GHz and 3.7 GHz. The 400 MHz bandwidth was unaffected by the considerable reduction in mutual coupling caused by the introduction of the S-shaped EBG structure. For the intended frequency band of the G slot MIMO antenna with EBG, the ECC value is less than 0.0002, and the diversity gain is larger than 9.99 dB. Its efficiency is more than 77%, and gain is more than 2.5 dB for a proposed frequency band. The simulation outcomes and the results from the fabricated antenna agree well. It is perfect for 5G n78 band operations.

REFERENCES

1. Puri, V. and H. S. Singh, "Design of an isolation improved MIMO antenna using metasurface based absorber for wireless applications," *Optik*, Vol. 259, 168963, 2022, https://doi.org/10.1016/j.ijleo.2022.168963.
2. Mohsenifard, F., A. Mahmoodzadeh, and Z. Adelpour, "Compact self-isolated four-element MIMO antenna for WLAN and ISM bands application," *IEEE Access*, Vol. 11, 9483–9492, 2023, doi: 10.1109/ACCESS.2022.3223133.
3. Kumar, P., S. Pathan, O. P. Kumar, et al., "Design of a six-port compact UWB MIMO antenna with a distinctive DGS for improved isolation," *IEEE Access*, Vol. 10, 112964–112974, 2022, doi: 10.1109/ACCESS.2022.3216889.
4. Babu, S. S. and S. R. Patre, "Meandered-line folded antenna for sub-6 GHz supported MIMO system," *2022 3rd International Conference for Emerging Technology (INCET)*, 1–4, Belgaum, India, 2022, doi: 10.1109/INCET54531.2022.9824239.
5. He, D., Y. Chen, and S. Yang, "A low-profile triple-band shared-aperture antenna array for 5G base station applications," *IEEE Transactions on Antennas and Propagation*, Vol. 70, No. 4, 2732–2739, Apr. 2022, doi: 10.1109/TAP.2021.3137486.
6. Yuan, X.-T., Z. Chen, T. Gu, and T. Yuan, "A wideband PIFA-pair-based MIMO antenna for 5G smartphones," *IEEE Antennas and Wireless Propagation Letters*, Vol. 20, No. 3, 371–375, Mar. 2021, doi: 10.1109/LAWP.2021.3050337.
7. Kshetrimayum, R. S., M. Mishra, S. Aïssa, S. K. Koul, and M. S. Sharawi, "Diversity order and measure of MIMO antennas in single-user, multiuser, and massive MIMO wireless communications," *IEEE Antennas and Wireless Propagation Letters*, Vol. 22, No. 1, 19–23, Jan. 2023, doi: 10.1109/LAWP.2022.3200483.
8. Ye, Y., X. Zhao, and J. Wang, "Compact high-isolated MIMO antenna module with chip capacitive decoupler for 5G mobile terminals," *IEEE Antennas and Wireless Propagation Letters*, Vol. 21, No. 5, 928–932, May 2022, doi: 10.1109/LAWP.2022.3152236.
9. El-Din, M. S. H. S., S. I. Shams, A. M. M. A. Allam, A. Gaafar, H. M. Elhennawy, and M. Fathy Abo Sree, "SIGW based MIMO antenna for satellite down-link applications," *IEEE Access*, Vol. 10, 35965–35976, 2022, doi: 10.1109/ACCESS.2022.3160473.
10. Cheng, B. and Z. Du, "Dual polarization MIMO antenna for 5G mobile phone applications," *IEEE Transactions on Antennas and Propagation*, Vol. 69, No. 7, 4160–4165, Jul. 2021, doi: 10.1109/TAP.2020.3044649.
11. Zhang, H. H., G. G. Yu, X. Z. Liu, et al., "Low-SAR MIMO antenna array design using characteristic modes for 5G mobile phones," *IEEE Transactions on Antennas and Propagation*, Vol. 70, No. 4, 3052–3057, Apr. 2022, doi: 10.1109/TAP.2021.3121174.
12. Zhang, H. H., X. Z. Liu, G. S. Cheng, Y. Liu, G. M. Shi, and K. Li, "Low-SAR four-antenna MIMO array for 5G mobile phones based on the theory of characteristic modes of composite PEC-lossy dielectric structures," *IEEE Transactions on Antennas and Propagation*, Vol. 70, No. 3, 1623–1631, Mar. 2022, doi: 10.1109/TAP.2021.3133432.
13. Dilli, R., "Analysis of 5G wireless systems in FR1 and FR2 frequency bands," *2020 2nd International Conference on Innovative Mechanisms for Industry Applications (ICIMIA)*, 767–772, Bangalore, India, 2020, doi: 10.1109/ICIMIA48430.2020.9074973.
14. Sudhamani, et al., "A survey on 5G coverage improvement techniques: Issues and future challenges," *Sensors 2023*, 1–47, 2023, https://doi.org/10.3390/s23042356.
15. Sandi, E., A. Diamah, and M. A. Mawaddah, "High isolation MIMO antenna for 5G C-band application by using combination of dielectric resonator, electromagnetic bandgap, and defected ground structure," *EURASIP Journal on Wireless Communications and Networking*, 1–13, 2022, https://doi.org/10.1186/s13638-022-02208-1.
16. Ayalew, L. G. and F. M. Asmare, "Design and optimization of pi-slotted dual-band rectangular microstrip patch antenna using surface response methodology for 5G applications," *Heliyon*, Vol. 8, No. 12, e12030, 2022, doi:/10.1016/j.heliyon.2022.e12030.

17. Megahed, A. A., M. Abdelazim, E. H. Abdelhay, and H. Y. M. Soliman, "Sub-6 GHz highly isolated wideband MIMO antenna arrays," *IEEE Access*, Vol. 10, 19875–19889, 2022, doi: 10.1109/ACCESS.2022.3150278.
18. Ye, Y., X. Zhao, and J. Wang, "Compact high-isolated MIMO antenna module with chip capacitive decoupler for 5G mobile terminals," *IEEE Antennas and Wireless Propagation Letters*, Vol. 21, No. 5, 928–932, May 2022.
19. Ren, Z., A. Zhao, and S. Wu, "MIMO antenna with compact decoupled antenna pairs for 5G mobile terminals," *IEEE Antennas and Wireless Propagation Letters*, Vol. 18, 1367–1371, 2017.
20. Yuan, X.-T., Z. Chen, T. Gu, and T. Yuan, "A wideband PIFA-pair-based MIMO antenna for 5G smartphones," *IEEE Antennas and Wireless Propagation Letters*, Vol. 20, No. 3, 371–375, Mar. 2021.
21. Salah El-Din, M. S. H., S. I. Shams, A. M. M. A. Allam, et al., "SIGW based MIMO antenna for satellite down-link applications," *IEEE Access*, Vol. 10, 35965–35976, Apr. 2022.
22. Babu, S. S. and S. R. Patre, "Meandered-line folded antenna for sub-6 GHz supported MIMO system," *International Conference for Emerging Technology*, Belgaum, India, May 27–29, 2022.
23. Kshetrimayum, R. S., M. Mishra, S. Aïssa, et al., "Diversity order and measure of MIMO antennas in single-user, multiuser, and massive MIMO wireless communications," *IEEE Antennas and Wireless Propagation Letters*, Vol. 22, No. 1, 19–23, Jan. 2023.
24. Cheng, B. and Z. Du, "Dual polarization MIMO antenna for 5G mobile phone applications," *IEEE Transactions on Antennas and Propagation*, Vol. 69, No. 7, 4160–4165, Jul. 2021.
25. Kumar, P., S. Pathan, O. P. Kumar, et al., "Design of a six-port compact UWB MIMO antenna with a distinctive DGS for improved isolation," *IEEE Access*, Vol. 10, 112964–112974, Nov. 2022.
26. Suresh Babu, N., A. Q. Ansari, B. K. Kanaujia, et al., "A two-port UWB MIMO antenna with an EBG structure for WLAN/ISM applications," *Materials Today: Proceedings*, Vol. 74, 334–339, Nov. 2023.
27. He, D., Y. Chen, and S. Yang, "A low-profile triple-band shared-aperture antenna array for 5G base station applications," *IEEE Transactions on Antennas and Propagation*, Vol. 70, No. 4, 2732–2739, Apr. 2022.